Heliyon 9 (2023) e20542

Contents lists available at ScienceDirect

Heliyon

journal homepage: www.cell.com/heliyon

Isosterism in pyrrole via azaboroles substitution, a theoretical investigation for electronic structural, stability and aromaticity

Safinaz H. El-Demerdash [a,*], Shaimaa F. Gad [b], Ibrahim M. El-Mehasseb [b], Khaled E. El-Kelany [c]

[a] Chemistry Department, Faculty of Science, Menoufia University, Shebin El-Kom, 32512, Egypt
[b] Chemistry Department, Faculty of Science, Kafrelsheikh University, 33516, Kafr el-Sheikh, Egypt
[c] Institute of Nanoscience and Nanotechnology, Kafrelsheikh University, 33516, Kafr el-skiekh, Egypt

ARTICLE INFO

Keywords:
N-B doping
Isosteres
Aromaticity
DFT
Stability and azaboroles

ABSTRACT

This work uses ab-initio CBS-QB3 and density functional theory (B3LYP) to analyze the structure, stability, and aromaticity of all isosteric nitrogen-boron pyrroles. The mono-NB unit substituted group of the isosteric NB pyrrole has four isosteres, whereas the multi-NB unit substituted group has two isosteres. These two groups make up all isosteric NB pyrrole. For structural, energetic, magnetic, and electron delocalization criteria, the results highlight the predominance of the **PN3B2** isostere and its greater stability over other conformers. In addition, the global reactivity indices, ESP, HOMO-LUMO, and NBO charges have all been estimated to forecast the active side's electron donation and acceptance. These isosteres are categorized as weak electrophiles and marginal nucleophiles. NB-isosteres have poorer stability, HOMO-LUMO gap, and aromaticity than the parent (pyrrole). In general, NB compounds with more ring sharing are less aromatic than NB molecules with less ring sharing. The current study is anticipated to help in understanding of the chemistry of NB substituted molecules and their experimental identification and characterization.

1. Introduction

For describing the similarity of many structures with the same number of atoms and valence electrons, the term "isosterism" was employed. The identical net charge isosteres exhibit comparable physical and chemical characteristics [1]. The R3B-NR3 compounds have many interests in these structures where one or more C–C pair have been replaced by an NB unit [2–13]. The so-called electron deficiency of the boron atom governs its chemistry in molecular systems when nitrogen and boron are bound together [7]. Inorganic materials, such as B–O and N–B compounds, have great oxidation resistance, high thermodynamic stability and are more rigid at high temperatures [14–16]. The resonance stabilization in a variety of systems, including boron-nitrogen coronenes, borazenes, phosphazenes, and boron-phosphorous nanographene-like material, has been linked to this high stability [13,17,18].

Because of the polarity of the NB unit, these compounds have special electrical properties that could find use in a variety of industries, including biomedicine [19], hydrogen storage in combustion cells [20–24], organic electronics [25–27], and synthetic chemistry [28]. The orientation, number, and position of NB group in conjugated organic structures having more than one NB pair are thought to have interested effects on their intermolecular chemical reactions and structural electronic properties due to the

* Corresponding author.
E-mail address: hamdysafinaz@yahoo.com (S. H. El-Demerdash).

https://doi.org/10.1016/j.heliyon.2023.e20542
Received 4 May 2023; Received in revised form 26 August 2023; Accepted 28 September 2023
Available online 29 September 2023
2405-8440/© 2023 Published by Elsevier Ltd. This is an open access article under the CC BY-NC-ND license (http://creativecommons.org/licenses/by-nc-nd/4.0/).

isoelectronic correlation among the nitrogen-boron (NB) unit and the carbon-carbon (CC) unit. The class of organic compounds known as nitrogen-boron doped π-conjugated complexes has been hailed as having remarkable electrical and optical properties that play important role in optoelectronic devices [25–27].

Several NB-doping compounds have been synthesized, including mono NB-substituted analogues of benzene [29–31], NB indoles, boron nitride-fused cyclamens [2], cyclo-BN-tetracene, and cyclo-BN-anthracene [32]. Dissecting the essential characteristics of nitrogen boron heterocycles, for example, stability, conformation, aromaticity, and molecular orbital energies, has received special attention [33–40].

Furthermore, numerous studies have considered the influence of incorporating Boron Nitrogen into fullerene and nanotube frameworks [41–43]. The introduction of hetero-atoms such as boron or nitrogen into carbon nanotubes offers the possibility of tailoring their structural and electronic properties. When a foreign atom is inserted in the nanotube lattice, the nanotube symmetry is altered and its structure and properties consequently change. So, it is important to take into account both NB substitutions in five-membered rings as well as six-membered rings. A cyclopentadiene analogues with two NB units was first approach by Roesler and co-workers [6,44]. The molecular and physical characteristics of unique azaborole heterocycles were studied computationally. The azaboroles (five membered ring) are stable in dry surrounding and have an untapped possibility as innovative essential part towards the investigation of novel drug-like structures and substances. In this study, only two isosteres of NB mono substituted furan, thiophene, and pyrrole have been investigated [45].

The most prevalent heterocyclic aromatic organic molecule with a five-membered ring and nitrogen heteroatoms in our system is pyrrole (C4H5N). It is a white, flammable liquid that can be found in skin, bone oil, and the amino acids proline and hydroxyproline found in ligaments [46]. Several naturally occurring compounds [47] and biologically active chemicals [48] have its structural components. Since the synthesis of 1,2-azaborine (2008), the idea of replacing C═C bonds by isoelectronic boron – nitrogen bonds have attracted new attention and is currently being investigated for use in the pharmaceutical and material sciences.

This paper will concentrate on six completely alternated NB-pyrrole compounds with nitrogen and boron. According to our knowledge, this is the first systematic investigation to encompass various NB doping methods for pyrrole. The goal is to use DFT and composite quantum chemical approaches to discuss fundamental features such as electronic structures, stability, reactivity, and aromaticity.

1.1. Theoretical methods

All quantum chemical measurements were done by Gaussian 09 [49], where the geometries of different structures were performed using GaussView 5.0.9 [50] and chemcraft 1.6 [51] programmes. The B3LYP [52,53] method with 6-311 + G(d,p) basis set [54] and a high level composite CBS-QB3 [55] are used. Then, single point calculations by using the B3LYP/6-311 + G(d,p) geometries were carried out at CCSD (T)/6-311 + G (d,p). Each stationary point has undergone frequency calculations to determine whether it is a minimum or transition state, where no negative frequencies have been identified.

Chemical global reactivity descriptors [56–58] have been measured using the energies of HOMO and LUMO (the highest occupied and lowest unoccupied molecular orbitals, respectively) to comprehend the reactivity and stability of the examined structures. Hardness (η), softness (S), ionization potential (IP), electron affinity (EA), electronegativity (χ), electrophilicity (ω), nucleophilicity (N) were calculated at B3LYP/6-311 + G in accordance with Koopmans' theorem [59]. The files exported by Multiwfn software were used to plot the electrostatic potential (ESP) surfaces and the scanning tunnelling microscopy (STM) images for all isosteres [60].

The global descriptors for chemical reactivity have been performed using the following equations:

$$\eta = \frac{1}{2}(\mathbf{IP} - \mathbf{EA}) \tag{1}$$

$$S = 1/2\eta \tag{2}$$

$$IP = -E_{HOMO} \tag{3}$$

$$EA = -E_{LUMO} \tag{4}$$

$$\chi = \frac{1}{2}(\mathbf{IP} + \mathbf{EA}) \tag{5}$$

$$\boldsymbol{\omega} = \boldsymbol{\mu}^2 / \mathbf{2\eta} \tag{6}$$

$$\mathbf{N} = \mathbf{1} / \boldsymbol{\omega} \tag{7}$$

The natural bond orbital analysis (NBO) was calculated at B3LYP/6-311 + G(d,p) to determine the charges of different atoms, their effects on stability and orbital interactions using the NBO programme version 3.1 [61]. On the natural atomic orbital NAO basis, the Laplacian bond order and decomposed Wiberg bond order have also been computed.

In this research, we applied six indicators of aromaticity calculated at B3LYP/6-311 + G(d,p) level. The B3LYP functional have been selected since, it is found to be one of the most appropriate method for describing the aromatic hydrocarbons properties and stability [62–65]. The Nucleus independent chemical shift (NICS) is the magnetic criteria of aromaticity [66–69] proposed by Schleyer et al.

The -ve value of the absolute shielding calculated at the center of the ring (NICS (0)) or at 1.0 Å above the system (NICS(1)). These values are measured at B3lyp/6-311 + G(d,p) using the gauge including atomic orbital (GIAO) method [70].

HOMA, the Harmonic Oscillator Measure of Aromaticity [71,72], and LOLIPOP, the Localized Orbital Location Integrated Over Plane [73], a geometry-based index, are alternative criteria for aromaticity that have been calculated. The degree of electron delocalization was estimated on the basis of the aromatic fluctuation index (FLU) and (FLU-π) which are based on π-atomic valence [74,75], concerns with the electron sharing amount between bonded pairs of neighbor atoms.

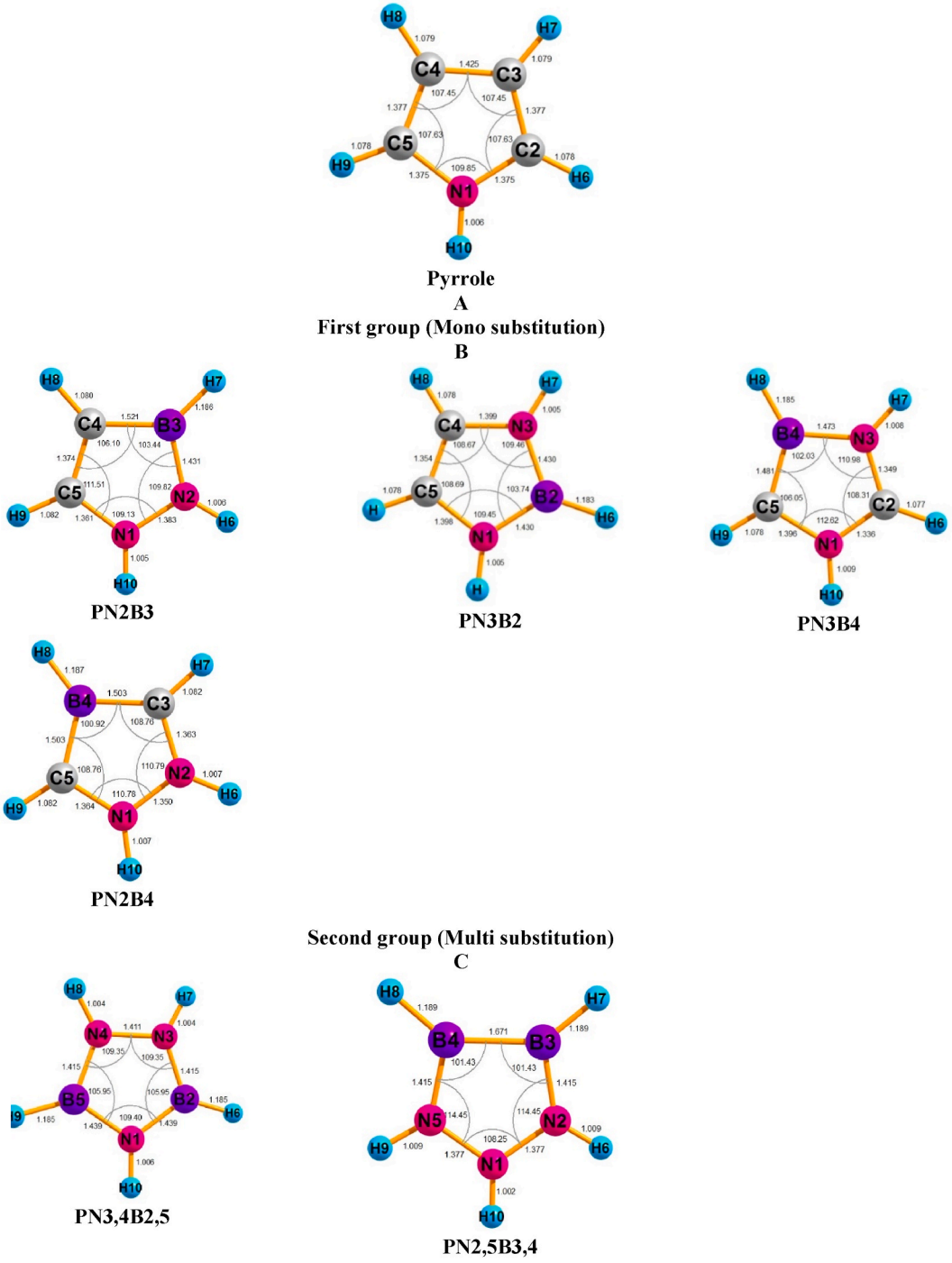

Fig. 1. Numbering and Optimized structures of pyrrole and its six NB isosteres with their corresponding geometrical parameters (in Angstroms and degree) at B3LYP/6-311 + G (d,p). Panel A depicts the parent (pyrrole), panel B the first group, and panel C the isosteres of the second group.

The goal of the multicenter delocalization indices (MCI) [76,77] is to measure the electron delocalization between different numbers of atoms. Several partitioning techniques can be used to determine the MCI [78–80]. In this study, MCI was calculated using the natural atomic orbital (NAO) analysis that were acquired from NBO results [81,82]. AV1245 [83] and the normalized multicenter bond order (NMCBO) index were used to evaluate MCI. Using the Multiwfn program, the geometry and electron delocalization criteria of the given aromaticity indices have been calculated.

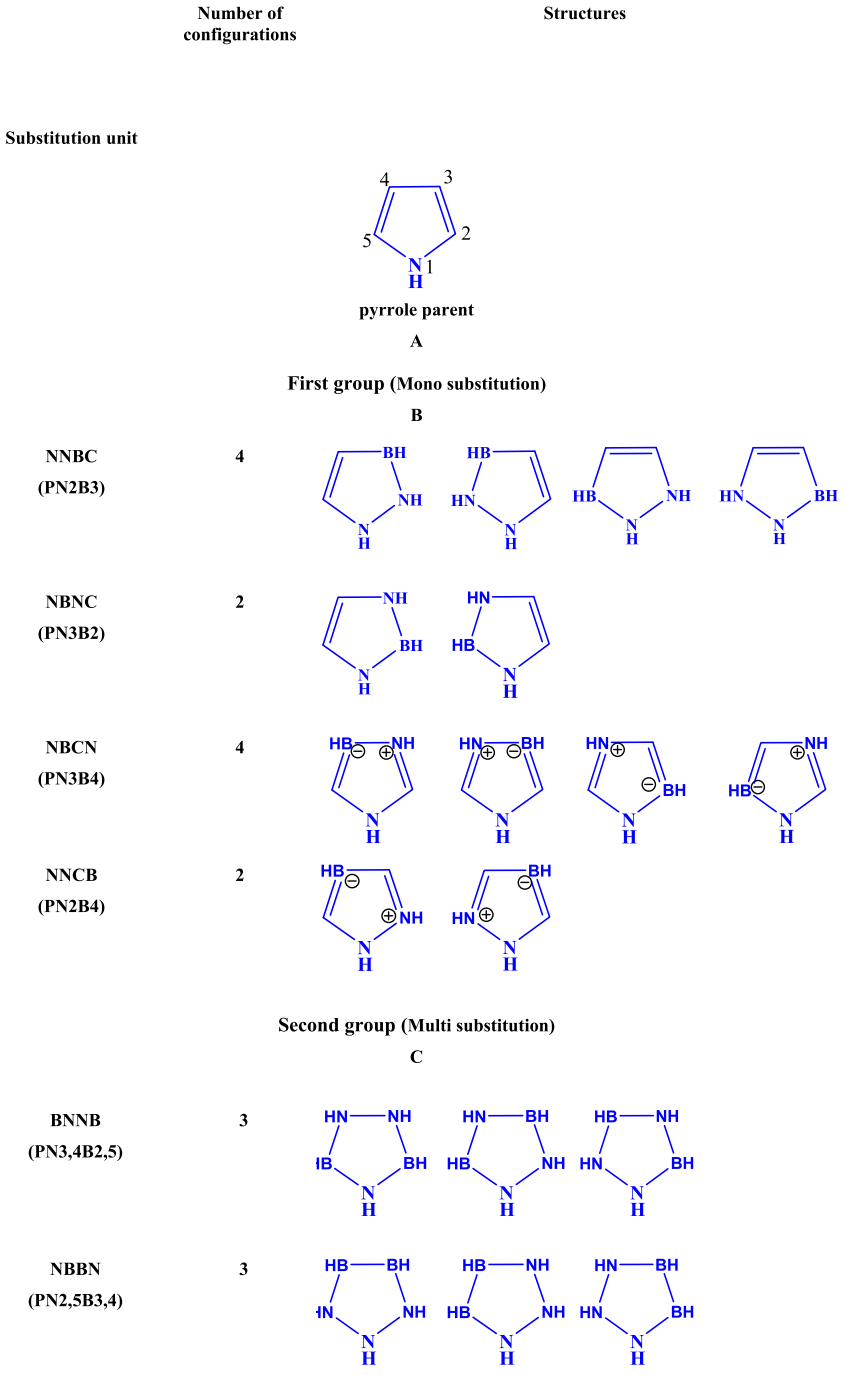

Fig. 2. Structures and substitution unit of different configuration for NB Pyrrole isosteres. The parent (pyrrole) is shown in panel A, first group is shown in panel B, and second group isosteres is depicts in panel C.

Table 1
Partial atomic natural charges (NPA) of NB Pyrrole isosteres at B3LYP/6-311 + G (d,p).

Atom number Isosteres	N1	N2	N3	N4	N5	B2	B3	B4	B5	C2	C3	C4	C5
Pyrrole													
P	−0.534	–	–	–	-	–	–	–	–	−0.056	−0.295	−0.295	−0.056
First group													
PN2B3	−0.421	−0.612	–	–	–	–	0.452	–	–	–	–	−0.575	0.021
PN3B2	−0.785	–	−0.785	–	–	0.584	–	–	–	–	–	−0.078	−0.078
PN3B4	−0.496	–	−0.721	–	–	–	–	0.302	–	−0.407	–	–	0.169
PN2B4	−0.360	−0.360	–	–	–	–	–	0.041	–	–	−0.243	–	−0.243
Second group													
PN3,4B2,5	−1.031	–	−0.640	−1.031	–	0.633	–	–	0.633	–	–	–	–
PN2,5B3,4	−0.283	−0.611	–	–	−0.611	–	0.243	0.243	–	–	–	–	–

2. Results and discussions

The electronic structure, physical, and chemical properties of the NB doped pyrrole under consideration should be significantly influenced by the relative positions of the boron and nitrogen atoms in the N–B moiety. We have taken into account every conceivable arrangement in the current investigation. The numbering method utilized throughout the current work is shown in Fig. 1 in order to avoid repetition in the labelling of particular isosteres. Two groups make up the isosteric nitrogen boron pyrrole. A NB mono substitution, which only involves the replacement of (C–C) with N–B unit, is included in the first group. Such substitution will lead to an overall 12 configurations. These twelve configurations are reduced to only four nonequivalent isosteres, see Fig. 2. The second group contains 6 configurations in all with only two independent isosteres uniquely the two isosteres will possess the units NBBN and NBNB. For ease of use, the PNn1Bn2 notation will be applied throughout the work where, P refers to the parent compound (pyrrole), n1 denotes substitution position for N and n2 for B atoms. Notably, n_1 and n_2 will be represented by one and two numbers, for mono and double substitution, respectively. For example, PN2B3 indicates that nitrogen is in position 2 and boron is in position 3. Similar to PN3,4B2,5, where boron and nitrogen atoms take the place 2,5 and 3,4 positions, respectively. The isosteres of NB pyrrole are **(PN3B2–PN3B4 – PN2B3 – PN2B4 – PN3,4B325 – PN2,5B3,4)**. For comparison, the results of an organic system (pyrrole) are also presented.

2.1. Geometries optimization

Fig. 1 displays the B3LYP/6-311 + G(d,p) optimized geometries for the parent pyrrole and its NB isosteres. A comparison between the experimental and literature data must be made to show the validity of the results gathered. The estimated geometrical characteristics of pyrrole and the corresponding values given [45,84] are in good agreement. The geometrical characteristics of the optimized NB isosteres at B3LYP/6-311G+(d,p) showed that the rearrange of the σ and π bonds along the molecule occurs in conjunction with the N–B doping processes.

All isosteres are non-planar after complete geometry optimization with the exception of **PN3B2** and **PN3B4** isosteres. The length of N–B bonds is in the range of 1.41 Å to 1.48 Å. This indicates aromaticity. For all NB isosteres, the length of N–B bond lies between the single and double bonds. A single N–B bond is in the range 1.56 Å and 1.66 Å [85–87], and a double N═B bound is between 1.34 Å and 1.41 Å [88]. The average N–B bond length in this investigation is 1.44 Å, which is comparable to the value for borazine (1.43 Å) [89,90].

The N1–C2 and N1–C5 bonds in the NB Pyrrole system shrink by 0.004 Å except in the **PN3B2** and **PN3B4** isosteres, where their bonds elongate by 0.021 Å. The length of the C–C bond lies between 1.35 Å and 1.42 Å, the C–N bond falls between 1.34 Å and 1.39 Å, the C–B bond lies within 1.34 Å and 1.50 Å, and the N–B bond is located around 1.41 Å and 1.47 Å. Based on these findings, C–N and N–B bonds resemble C–C bonds, while the C–B bond being slightly larger. In addition, the N–B bond is 0.016 Å to 0.12 Å times bigger than the N–N bond. The C–B bond length is also larger than that of the C–N bond from 0.31 to 0.16 Å. It worth noting that in NB structures, the intra-ring distances of the first group is smaller than the second one. So, the aromatic character of the first group is more than the second (see Fig. 1).

We can do compare the angles between C2C3C4, N3B4N5 and B2N3B4. In general, the CCC ≈107.6°, NBN ≈105.9°, and BNB ≈109.4, respectively. The occurrence of a lone pair of nitrogen atoms and the different atomic radii between boron and nitrogen could be related to the difference between these angles. The electronic pair, which is a crucial component of the link between the Lewis pairs, may be the reason why the CCC angle is less than BNB. The CCC angle is larger than NBN due to internal angles accommodation in the five membered ring. For **PN2B4** and **PN3B4** isomers, the N2C3B4 angle is increased by 1.3° than the C2C3C4 angle of pyrrole and the B2C3N4 is decreased by 1.4° while the angle (C2N3B4) of **PN3B4** isomer is 3.5° larger than the same angle. Our findings on the geometry of the **PN2B3** and **PN3B2** isomers are in good accordance with earlier calculations made at B3LYP/6-31 + G(d) [45].

2.2. Charge distribution

Table 1 contains the results of the natural population analysis (NPA) for the parent pyrrole (P) and its regarded isosteres According to an examination of such data, heteroatom nitrogen and carbon atoms are the principal targets of the negative charge. These will be the best sites for electrophiles. In contrast, boron atoms have a concentrated positive charge in line with their electronegativity.

Table 2
The total energies E_0 (au) and zero-point corrected relative energies ΔE_0 (kcal/mol) of NB Pyrrole isosteres at the three different methods.

Methods / Isosteres	CBS-QB3		B3LYP/6-311 + G(d,p)		CCSD(T)/6-311 + G(d, p)	
	E_0	ΔE_0	E_0	ΔE_0	E_0	ΔE_0
Pyrrole	−209.78647		−210.14434		−209.66103	
First group						
PN2B3	−213.18877	42.879	−213.55554	40.970	213.05709	44.663
PN3B2	−213.25710	0	−213.62083	0	−213.12826	0
PN3B4	−213.20722	31.305	−213.57230	30.452	−213.07781	31.660
PN2B4	−213.13733	75.159	−213.50414	73.223	−213.00643	76.455
Second group						
PN3,4 B2,5	−216.70010	0	−217.07099	0	−216.56634	0
PN2,5B3,4	−216.57316	79.659	−216.94608	78.381	−216.41861	92.703

Nucleophiles will consequently target these sites.

Table 1 shows that carbon and heteroatoms (nitrogen) have negative charge. So, these atoms will be the ideal locations for any electrophiles. On the other hand, boron atoms have a concentrated positive charge. As a result, nucleophiles will prefer the boron atoms. These results are demonstrated according to the electronegativity of nitrogen and boron atoms. The carbon atom's negative charge is the result of sharing of an electronic lone pair and bonds in resonance. The **PN3,4B2,5** isomer has the most negatively charged N atoms and the most positively charged B atoms. Due to the B atom is between two nitrogen atoms.

In accordance with the charge of pyrrole, **PN2B3** and **PN3B2** at the same level, NPA produces good findings [45.92]. The **PN2B4** isostere, which is obviously the least stable among the first group, has B and N atoms with less positive and less negative charges, respectively. The presence of a carbon atom between the N–B pair results in NB pair separation, is the cause of this decreased stability.

3. 3. Energies and stability

The difference between the total energies of isosteres and the most stable one is known as the relative energy ΔE_0. For instance, since **PN3B2** is the first group's most stable isostere, ΔE_0 of this group can be computed as $\Delta E_0 = E_{isoster} - E_{\mathbf{PN3B2}}$. Table 2 collects the total energy and zero point corrected relative energies at three distinct levels. Results from, B3LYP/6311 + G(d,p), CCSD(T)/6-311 + G (d,p) and CBS-QB3 show good agreement in reproducing ΔE_0 for pyrrole and NB substituted isomers, with the latter technique performing somewhat better. We shall therefore continue our discussion at the CBS-QB3 [91,92].

Passing from the parent pyrrole, the first group (mono NB replaced), and the second group (multi-NB substituted) results in an increase in the overall energy values This demonstrates that pyrrole is stabilized by NB substitution. The energy difference between pyrrole and it's the most stable isostere of first group is almost lower 50% than the second group at the same level. The nitrogen atoms' lone pair boosts electron density, which enhances resonance around our system's rings and results in a more stable molecule.

The following order of stability that depends on the energies is denoted as: first group (**PN3B2 > PN3B4 > PN2B3 > PN2B4) and second group (PN3,4 B2,5 > PN2,5B3,4**) by the ab initio method CBS-QB3. The instability of the **PN2B4 and PN2,5B3,4** isomers initiated by steric repulsion between the two lone pairs of connected two nitrogen atoms and the π-electronic system. The **PN2B3, and PN3,4B2,5** isomers have the lower repulsion, since the substituted nitrogen atom far enough from the nitrogen atom of pyrrole (N1).

According to an investigation of Hirshfeld partial atomic charges in the parent pyrrole (Fig. 3), the meta carbon position (C3 and C4) atoms have a higher negative charge than the ortho position (C2 and C5). If we had to replace the carbon - carbon bond with N–B unit, there would be preferable to place the more electronegative nitrogen in the 3 and 4 positions, while the less electronegative boron in the 2 and 5 positions instead of using different arrangements Hence, in the second group, the **PN3,4B2,5** isostere is the most stable one since it has an ortho position for boron and a meta position for nitrogen. Also, for the first group, **PN3B4** and **PN3B2** isomers are the most stable isosteres where the nitrogen atom is in a meta position.

We conclude that replacing a carbon atom in pyrrole with a nitrogen atom further polarizes the system, and the resulting charge distribution may help identify the best locations for the incoming boron atom. Thus produced 2-azapyrrole (pyrazole), 3-azapyrrole (imidazole), and 1,2,4-azapyrrole cations' most positive locations are depicted in Fig. 3. By taking into account the fact that the boron atom tends to be positioned at less electronegative sites, the stability trend of different isosteric NB pyrroles may be predicted. Starting with the 3-azapyrrole cation (imidazole), the position 2 would be the most preferred location for boron, and the **PN3B2** isostere is in fact the most stable among the first group. The same study starting with the pyrazole cation predicts the most preferred site for boron to give **PN2B4** (75.16 kal/mol), **PN2B3** (42.87 kcal) isosteres at CBS-QB3. In this case as well, the stability is decreased by replacing the carbon atom in positions 3 and 4 by a boron atom. If we began with the 1,2,4-azapyrrole cation, the second group has the highest observed and predicted stability for **PN3,4B2,5** isostere.

For each group produced from pyrazole-H^+, immidazole-H^+, and 1,2,4-azazpyrrole cations, we came to the conclusion that the stability order of NB inorganic pyrrole is connected to charges of boron and nitrogen atoms. The energy of the structures increases when the nitrogen and boron have less negative and positive charges respectively. Adding boron atoms to the ortho locations 2 and 5 and nitrogen atoms to the meta positions 3, 4 results in another stabilization of the structure, and the electronic pair of nitrogen atoms increases the electron density, improving the ring resonance as a result.

3.1. Thermodynamic properties

All the thermodynamic results give useful data for the study of thermodynamic energies and determine directions of chemical reactions based on the second law of thermodynamics. The values at normal pressure and room temperature of thermal energy (E),

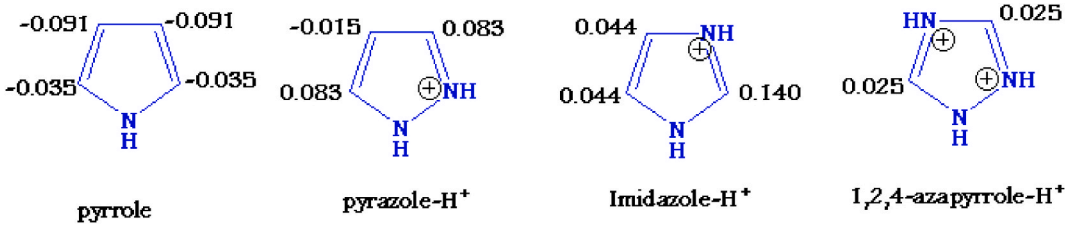

Fig. 3. Hirshfeld partial atomic charges in Pyrrole, protonated pyrazole, imidazole, and 1,2,4 azapyrrole cations.

Zero vibrational point energy (ZPVE), Gibbs free energy (G), Constant Volume Heat Capacity (Cv), Entropy (S), Enthalpy (H), were calculated are calculated by B3LYP and MP2 method using 6-311 + G(d,p) and 6-311 + G (2df, 2p) as basis set, respectively. The results are recorded in Table 3.

It is noted that these parameters are more indispensable with the NB isosteres. We observed that thermal energy (E) of the NB-pyrrole isosteres is lower than that organic pyrrole, while the entropy and Constant Volume Calorific Capacity of the doped isosteres is higher than that of the parent molecule (pyrrole), which confirms, the charge dynamics of the NB-doped structures are higher than its original molecule at the same pressure and temperature. This is because of the NB bond is more electronegative than CC unit. This results further demonstrates that NB isosteres have a high chemical reactivity and a high thermal resistivity.

Concerning the Gibbs free energy, it is an essential parameter for the thermodynamic stability of a molecule at a room temperature T and pressure P. Lower the Gibbs free energy, the more stability of the isostere. The values of G in Table 3 show a strong decrease during doping moving from parent, mono N substituted to multi-NB substituted. The lowest value for first group isostere is **PN3B2 (**−213.131166 au), and the lowest value for second group is PN**3,4B2,5** (−216.573011 au) at MP2. Therefore, these isosteres are the most thermodynamically stable doped. From our results, we notice that E, ZPVE, H, and G values decrease during doping from mono BN substituted to multi-BN substituted isosteres, on the other hand, the Cv and S values increase at the same level. In the first group isosteres, the most stable structures **PN3B2** and **PN3B4** have the lowest values of entropy 66.493 and 66.565cal/mol. Kelvin at MP2 respectively, while for the second group, the most stable isostere **PN3,4B2,5** has the largest constant volume calorific capacity 17.453 Cal / mol. Kelvin and the least stable isostere **PN2,5B3,4 has** the largest value of entropy 67.645 cal/mo. Kelvin at MP2.

In addition, the enthalpy of our doped structures is all negative, making it possible to conclude that they are thermodynamically stable. A similar behavior on the values of the thermal energy was observed and decreasing its values shown during doping confirms the improvement in the stability of the doped monomers. As regards the heat capacity, slight increases were observed during doping.

3.2. Dipole moments

The computed dipole moments of the investigated isosteres at various methods are shown in Table 4. According to our findings, the more precise electron correlated methods CCSD (T) and MP2 provide more accurate dipole moment estimates [92,93]. Dipole moments determined by B3LYP/6-311 + G (d,p) calculations are less than those predicted by MP2/6-311G(2df,2p) and CCSD (T)/6-31 + G calculations. These findings imply that the values of the computed dipole moments depend on the basis set chosen. As shown in Table 3, the dipole moment of NB-doped structures in the (0.474–4.86 D) range at MP2/6-311G (2df,2p). The lowest dipole moments at MP2 are 0.474 and 0.784 for the **PN3B2** and **PN3,4B2,5** isosteres, respectively. This is as a result of the two polar groups are in opposite orientations. See Fig. 1.

The existence of boron atoms adjacent to nitrogen atoms decreases the value of dipole moment due to the mutually charges (B, positive; N, negative). The calculated dipole moment of pyrrole is 1.4 times greater than **PN3B2** isostere which is the most stable one of the first group.

The highly polar molecules (**PN2B4**) demonstrate how is polar the N–B bond. The **PN2B4** isostere has the greatest dipole moment (4.87 D) at MP2/6-311G. (2df,2p). It should be observed that in this system, when the polar N atom and the polarized NH group place, this causes the overall dipole moment to increase. We conclude that the least stable isomer is more polar than the most stable one.

Table 3
Zero Vibrational Point Energy (ZPVE), Gibbs free energy (G), Thermal Energy (E), Constant Volume Calorific Capacity (Cv), Enthalpy (H), and Entropy (S), of the NB – substituted pyrrole isosteres using B3LYP/6-311 + G (d,p) method at constant temperature and pressure. Values in parentheses are calculated at MP2/6-311 + G (2df, 2p) method.

Parameters Isosteres	ZPVE (au)	G (au)	E (kcal/mol)	S (cal/mol. Kelvin)	H (au)	Cv (Cal/mol. Kelvin)
Parent (P)	−210.14830 (−209.63590)	−210.17404 (−209.66163)	54.087 (54.536)	64.525 (64.470)	−210.14338 (−209.63099)	14.824 (14.771)
First group						
PN2B3	−213.55980 (−213.03463)	−213.586430 (−213.06124)	52.381 (52.931)	66.993 (66.970)	−213.55459 (−213.02942)	16.106 (16.039)
PN3B2	−213.62500 (−213.10464)	−213.65155 (−213.13116)	52.813 (53.309)	66.652 (66.493)	−213.61988 (−213.09957)	15.917 (15.712)
PN3B4	−213.57647 (−213.05797)	−213.60300 (−213.08450)	52.574 (53.002)	66.590 (66.565)	−213.57136 (−213.05287)	15.998 (15.903)
PN2B4	−213.50863 (−212.98817)	−213.53541 (−213.01515)	51.987 (52.471)	67.786 (68.570)	−213.50320 (−212.98257)	16.792 (16.965)
Second group						
PN3,4B2,5	−217.07561 (−216.54669)	−217.10185 (−216.57301)	51.203 (51.746)	66.946 (67.235)	−217.07004 (−216.54106)	17.494 (17.453)
PN2,5B3,4	−216.95055 (−216.41453)	−216.97740 (−216.44132)	50.954 (51.612)	67.901 (67.645)	−216.94514 (−216.40918)	16.991 (16.654)

Table 4
Dipole moments (in Debye) for isosteres of NB-pyrrole.

Isomers	Methods		
	B3LYP/6-311 + G(d,p)	MP2/6-311G (2df,2p)	CCSD(T)/6-311 + G(d,p)
P	1.881	1.865	1.942
First group			
PN2B3	2.780	2.433	2.497
PN3B2	0.640	0.474	0.534
PN3B4	3.782	4.290	4.432
PN2B4	4.824	4.869	5.012
Second group			
PN3,4 B2,5	1.523	0.784	0.784
PN2,5 B3,4	4.733	2.300	2.346

3.3. Chemical reactivity

3.3.1. Theory of frontier molecular orbitals

To investigate the electronic structure and reactivity of organic compounds and to calculate the energy gap, this section focuses HOMO and LUMO, which are also known as frontier molecular orbitals (FMO) [94,95]. See Table 4. The molecules with high energy gap are less polarizable and their chemical reactivity is low and kinetic stability is high [96,97]. With the exception of **PN2B3** and **PN3, 4 B2,5** isosteres, the energy gap values in NB isosteres decrease when compared with the parent (pyrrole).

The least stable **PN2B4** isostere in the first group would be the most straightforward to ionize because it has the lowest energy HOMO orbital (−5.03 eV). The most stable isostere (**PN3B2**) has the highest E_{LUMO}, as was previously indicated (−0.013 eV). This illustrates that the electron-donating ability for NB doping of pyrrole is not strong. The **PN2B4** isostere's measured value (E gap = 4.73 eV) is lower than that of the **PN2B3** isostere (E gap = 6.06 eV). Hence, the **PN2B4** isostere has the highest interactions for intra-molecular charge transfer and is the most polarizable one (Table 5).

In the second group, the PN3,4B2,5 isostere is a hard molecule and has the least ability to polarize due to its higher energy gap (6.17 eV) than that of the PN2,5B3,4 (5.64 eV). The most stable PN3,4B2,5 isostere has the highest energy LUMO orbital (−0.091 eV) also has the highest energy of electron affinity (EA). So, this isostere has more tendency to attract a bonding pair of electrons. In another meaning, the compound is not easiest to loss or reduce electrons.

3.3.2. Electrostatic potential (ESP), HOMO and LUMO surfaces

To determine the distribution and symmetry of the frontier orbitals, HOMO and LUMO surfaces are essential. The HOMO and LUMO surfaces of the NB pyrrole isosteres as determined by the B3LYP/6-311 + G (d,p) level of theory are shown in Fig. 4. While the LUMO was delocalized over the whole N–H and C–H groups for the parent pyrrole, the HOMO was located over C═C groups.

The formation of the molecular orbitals isn't contributed equally for NB pyrrole isosteres due to the difference in electronegativity and the presence of one and two lone pairs of nitrogen. In the first group, the HOMO was localized on the N–B and C–C units or the C–N and C–B pairs, whereas the LUMO was localized on the N–H or C–H groups. In the second group, the HOMO was localized over the N–B groups while the LUMO was localized on the N–H or B–H groups. The HOMO-LUMO translation denotes an electron density transfer from C–N, C–B, and N–B groups to N–H and B–H.

As it is known, the electrostatic potential map (MEP) plays an important role in displaying the difference between sites for nucleophilic and electrophilic attack and is related to electronic density [98]. The electrostatic potential map of the studied molecules is shown in Fig. 5. The negative (high electron density) (red) regions of the MEP are related to nucleophilic reactivity and the positive (low electron density) (blue) regions are related to electrophilic reactivity.

From this figure, one can deduce that, the whole electron density is dispersed around the ring of the parent without any remarkable distortion. For the analysis of NB-pyrrole analogues, the more electron density (red color) areas are fundamentally focus around the

Table 5
Global chemical descriptor (eV) of the Studied Structures of NB-Pyrrole at B3LYP/6-311 + G (d,p).

Structures Parameters	Parent	First group				Second group	
	P	PN2B3	PN3B2	PN3B4	PN2B4	PN3,4 B2,5	PN2,5B3,4
E_{HUMO}	−5.947	−6.344	−5.580	−5.027	−5.383	−6.257	−6.529
E_{LUMO}	−0.084	−0.284	−0.013	−0.292	−0.698	−0.091	−0.894
E_g	5.862	6.059	5.567	4.734	4.684	6.165	5.635
IP	5.947	6.344	5.580	5.027	5.383	6.257	6.529
EA	0.084	0.284	0.013	0.292	0.698	0.091	0.894
X	3.016	3.314	2.797	2.660	3.040	3.174	3.712
η	2.931	3.029	2.783	2.367	2.342	3.082	2.817
S	0.170	0.165	0.179	0.211	0.213	0.162	0.177
ω	1.551	1.813	1.405	1.494	1.973	1.634	2.445
N	0.644	0.551	0.711	0.669	0.506	0.611	0.408

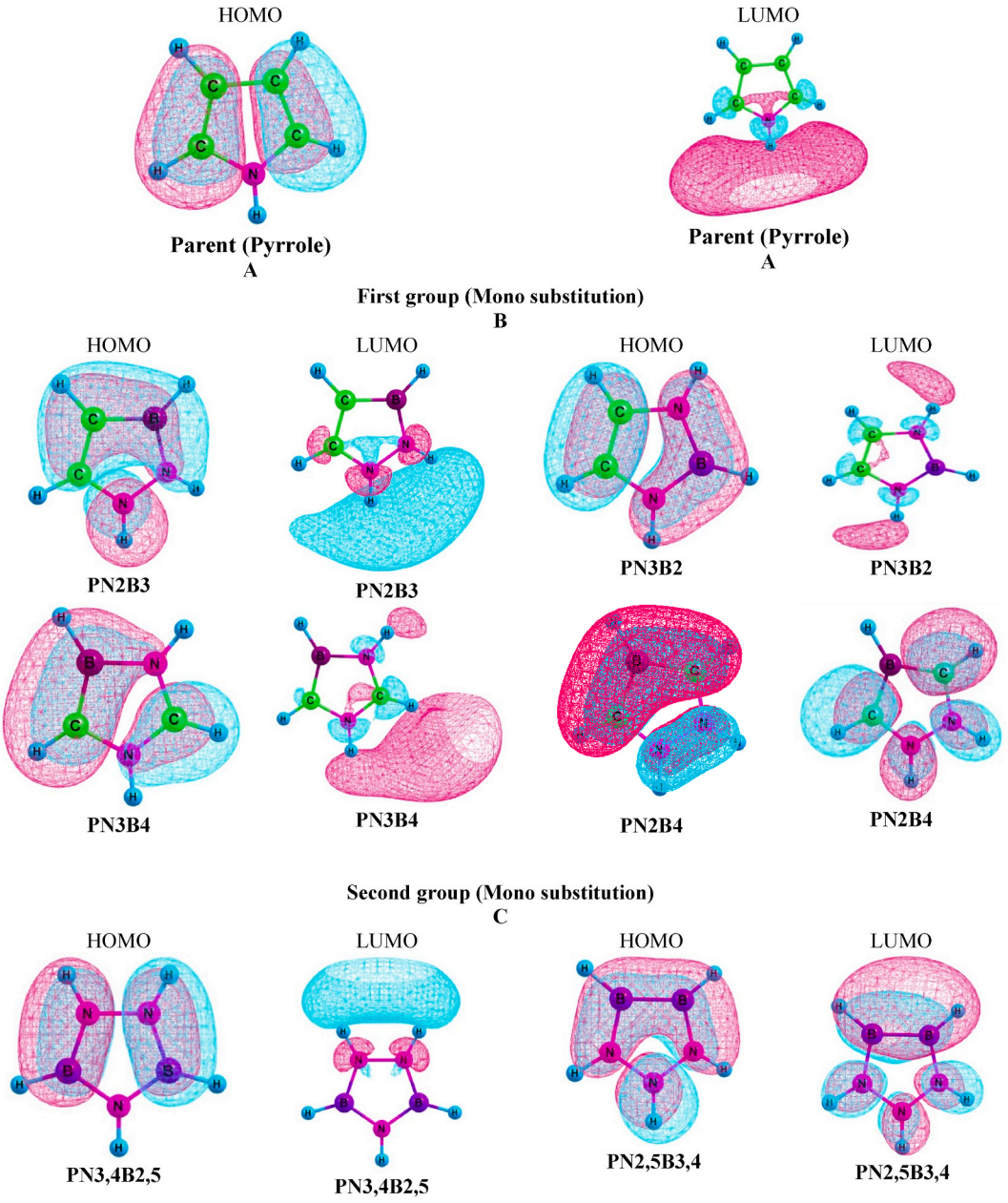

Fig. 4. Calculated highest occupied molecular orbital (HOMO) and lowest unoccupied molecular orbital surfaces of pyrrole and its NB analogues using B3LYP/6-311 + G (d,p). The parent (pyrrole) is depicted in panel A, the first group is depicted in panel B, and the second group isosteres are illustrated in panel C.

boron and carbon atoms attached to boron (C═C, C–B, C–H, and B–H). The poor electron density (blue color) regions are centralized around N–H groups.

The N–H sites are surrounded by blue color and this indicate that the electron density moves to the nitrogen atom during the excitation process. So, the boron atoms have the ability to donate electrons toward electrophiles, while the nitrogen atoms are more acidic. This means that the nitrogen atoms easily loss proton (the N atoms don't have significant abilities to form H-bonds) while, B atoms are believed to have the highest electron donation ability toward electrophiles (protons). Hence, boron atoms have a higher electron density in their ground state than their excited states of isomers, so nitrogen atoms have an excited electron density greater than their ground state.

3.3.3. Global indices of reactivity

The global reactivity of the investigated structures was noted in Table 5 in order to explore the effects of doping on the isoterism

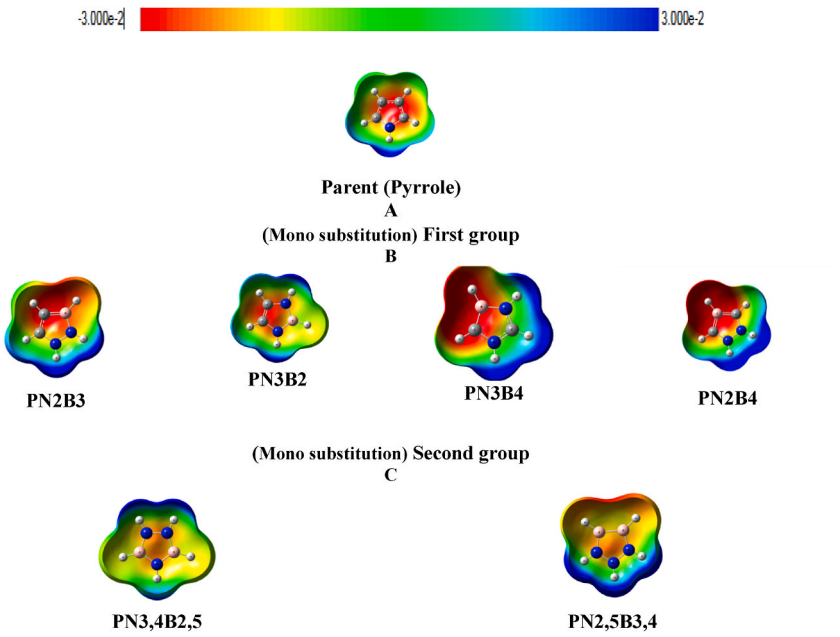

Fig. 5. Calculated electrostatic potential structures of pyrrole and its NB analogues using B3LYP/6-311 + G (d,p) level of theory. The parent (pyrrole) is shown in panel A, first group is shown in panel B, and second group isosteres are shown in panel C.

features and on the reactivity of our system. When the system resist to a change in its electrons number is expressed by chemical hardness (η) and global softness (σ) (see equations (1) and (2)). In these structures, when η is small value, the isostere is soft, and is called hard by increasing the value of hardness [99]. By comparing soft and hard molecules, the Eg is larger for the latter. The second group has the highest chemical hardness value (3.08), which indicates that the **PN3,4B2,5** isostere is very hesitant to exchange electron density with its surroundings.

The molecule with the large band gap is usually stable and unreactive, whereas those with smaller band gaps are reactive. We can draw the conclusion that for unimolecular reactions like isomerization and dissociation, hard molecules will be less reactive than soft molecules. Since the softness of the **PN2B3** and **PN3B2** isomers is significantly the same, adding a nitrogen atom to either 2 or 3 position has no effect on the softness of pyrrole. The reactivity of the isosteres is in decreasing order (PN2B4 > PN3B4 > PN3B2 > PN2,5B3,4> PN2B3 > PN3,4B2,5). The most reactive isostere is PN2B4, with a high value of softness of 0.21 eV. The electronegativity of NB isosteres is much higher than 3 eV except for (PN3B2, PN3B4) **it is** not much different. This is the energy midpoint between the E_{HOMO} and the E_{LUMO} for NB isosteres. We mean that the electronegativity value is the half of summation E_{HOMO} and E_{LUMO} for pyrrole and its NB isosteres based on equation (5)(See Table 5), where $\chi = \frac{1}{2}(\mathbf{E}_{HOMO} + \mathbf{E}_{LUMO})$. Equation (3) determines that the ionization potential of the least stable second group isosteres, PN2,5B3,4, is greater than that of the other isosteres and is 6.53 eV.

Table 6
Laplacian bond order and total Wiberg bond order (values are in parentheses) for NB isosteres of pyrrole at B3LYP/6-311 + G (d,p).

Structures	Bond order									
	C–C	C═C	C–H	C–N	C–B	N–H	B–H	N–B	N–N	B–B
Pyrrole	1.244 (1.319)	1.499 (1.567)	0.837 (0.931)	0.923 (1.185)	–	0.692 (0.810)	–	–	–	–
First group										
PN2B3	–	1.537 (1.689)	0.841 (0.925)	0.969 (1.156)	1.053 (1.091)	0.681 (0.816)	0.856 (0.975)	0.653 (1.100)	0.621 (1.044)	–
PN3B2	–	1.660 (1.695)	0.842 (0.931)	0.839 (1.124)	–	0.692 (0.817)	0.865 (0.978)	0.673 (1.065)	–	–
PN3B4	–	–	0.844 (0.937)	1.089 (1.278)	1.211 (1.384)	0.696 (0.812)	0.845 (0.978)	0.486 (0.955)	–	–
PN2B4	–	–	0.836 (0.930)	0.933 (1.220)	1.055 (1.291)	0.686 (0.801)	0.832 (0.975)	–	0.787 (1.099)	–
Second group										
PN3,4 B2,5	–	–	–	–	–	0.682 (0.818)	0.861 (0.972)	0.723 (1.022)	0.547 (1.041)	–
PN2,5 B3,4	–	–	–	–	–	0.686 (0.817)	0.847 (0.972)	0.681 (1.166)	0.606 (1.051)	1.082 (1.048)

Depending on the electrophilicity index value, organic compounds are categorized as powerful, modest, or misfit electrophiles. Strong electrophiles have ω > 1.5eV, modest electrophiles have a range of 0.8 < eV, and misfit electrophiles are <0.8 eV [100] using equation (6). While, molecules with a nucleophilicity index of N > 3.0 eV are powerful nucleophiles, 2.0 < N < 3.0 eV are modest, and those with N < 2.0 eV are misfit nucleophiles [101] see equation (7). The NB pyrrole analogues are strong electrophiles, except **PN3B2** and **PN3B4** isosteres, which are moderate electrophiles. The PN3B4 isomer has the highest nucleophilicity index of 0.920 eV. Hence all NB pyrrole analogues are marginal nucleophiles.

3.4. Laplacian bond order and wiberg bond order analysis

Bond order is a very useful and significant tool to characterize chemical bonding. Multiwfn software supports many bond order types. Different physical meanings are formed due to many bond orders. Such as, Laplacian bond order (LBO) describes the covalent bond component and it has a good correlation with bonding strength or bond dissociation energy. The Wiberg bond order describes the contributions decomposition from atomic orbital pairs. The Wiberg bond order values are larger than those of the LBO analysis at B3LYP/6–311+ G(d,p).

The LBO and **Wiberg bond orders** of different NB isosteres are presented in Table 6, and predict the same successive strength of the bonds in the arrange of C═C > C–C > C–B > C–N > B–H > C–H > N–H > N–B > B–B > N–N. This discovers the polarizability of these bonds [102], in the arrange of C–H > C–N > C–C > C═C.

3.5. Scanning tunnelling microscopy (STM)

Using the analysis of 2D surface covalent organic compounds and the evaluation of the bond order, the STM simulation was used to shed light on aromaticity [103,104]. The simulation, which was presented in Fig. 6, was run with voltage bias at −0.5 V and current at 1.2 A, respectively. This makes it possible to visualize the structure of covalent bonds directly [105]. The brilliance of these bonds reflects the higher electron density. In general, relative to other bonds, the molecules' C–C and C–B bonds exhibit greater brightness in the first group isosteres. The primary cause of this effect is an increase in electron density at these bonds due to the electronic delocalization in the conjugated system. In the second group's, the nitrogen atoms enhanced electron density may be seen because of their lone pair and smaller electrostatic and van der Waals forces.

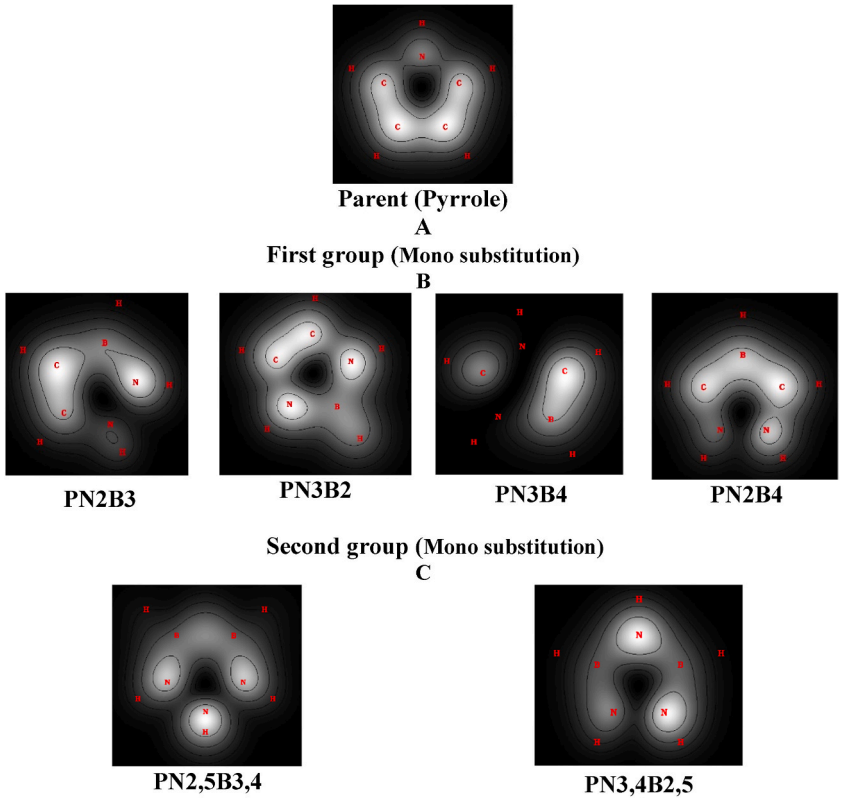

Fig. 6. STM diagram for pyrrole and its NB-isosteres. (A) Is the parent pyrrole, B is for first group, and second group isosteres are shown in panel C.

3.6. Aromaticity indices

Aromaticity is one of the most crucial characteristics to consider when assessing the reactivity organic structures [106]. We used six measures of aromaticity in this investigation. These descriptors' primary objective is measuring the amount of electron delocalization, which is associated with the ring's aromaticity.

3.6.1. Magnetic criteria

The ultimate magnetic shielding calculated at particular locations in the ring center close to the examined structures above it is known as the nucleus-independent chemical shifts (NICS). Table 6 provides four NICS indices for the NB pyrrole isosteres that were computed at the B3LYP/6-311 + G(d,p) level. Positive NICS values indicate anti-aromaticity, while zero NICS results in non-aromatic. Negative NICS values indicate aromatic character. NICS(0) denotes the isotropic shielding at the ring's center, while NICS(1) is that 1 Å above the center of the ring. The NICS(1)zz, one of the four NICS indices, will be utilized in further discussion since it provides a more precise measurement of magnetic shielding [107–111]. Our findings in Table 7 show a good agreement with earlier research on pyrrole [112–114].

The NICS(1)zz index suggests a similar aromaticity of the corresponding rings having the orientational isosteres for example, **PN2B3 – PN3B2** with values (−20.5–21.9) ppm and **PN2B4 – PN3B4** isosteres with (−28.2,- 27.1 ppm) respectively. The second group has the same value (−14.1 ppm). The organic pyrrole has a more negative value of NICS(1)zz (−31.02 ppm) than all NB inorganic isomers. The most stable isosteres for the first and second groups are **PN3B2** and **PN3,4B2,5** which have negative value of NICS(1)zz (−21.90 and −14.15 ppm) respectively.

The NICS(1)zz results of pyrrole is lightly higher range (70%–90%) for the first group NB-isosteres and is nearly double than that of the corresponding NB-isosteres of second group. Basically, these values refer to π bonds. The π bonds in pyrrole and inorganic isosteres are different because of the latter have π dative bonds (Lewis's acid and base). The NB - pyrrole isosteres are polar due to the electronegativity of boron and nitrogen atoms are different, and due to the sharing of the electronic lone pair of nitrogen atoms in the ring. The HOMO of NB-pyrrole is deformed (More intense around the nitrogen atoms). This points out the C–C bonds stronger than that of N–B bonds. Furthermore, there is a little extending of the ring of NB-system than that of pyrrole due to the characteristic of dative π bonds. Finally, the aromaticity decreases during substitution of a CC unit by a NB one. So, the second group is less aromatic than the first group. Clearly, the NICS values indicate organic parent (pyrrole) is more aromatic than NB doped isosteres.

3.6.2. Geometric criteria

The harmonic oscillator model (HOMA) is one of geometric criteria that is used to investigate aromaticity. When the value of HOMA increase, the ring becomes more aromatic, and more delocalized. The calculated HOMA values of NB pyrrole analogues, shown in Table 7, suggest that all NB isosteres display the aromatic character. According to the values, aromaticity generally decreases with increasing the number of NB unity. All the calculated HOMA values are smaller than 0.854, which indicate that the electronic delocalization is lower than parent, so all NB pyrrole analogues have smaller aromatic character than the parent (pyrrole). The aromaticity decreases in the order **(P > PN3B4 > PN3B2 > PN2B4 > PN2B3)** for the first group and **(PN3,4B2,5 > PN2,5B3,4)** for the second group. These results show a significant order with the relative energies of NB isomers.

In the investigated NB system, NICSzz and HOMA calculation were performed at the B3LYP/6-311 + G(d,p) level provide a good match with previous studies on pyrrole [115–117]. During moving from first group to second group isomers, both NICS (1) zz and HOMA indices show good results with the decreasing order of aromaticity. In NB pyrrole analogues, the five membered ring is distinguished by decreasing aromaticity specifically for the 2,3 and 2,4 NB-related species than for the 3,4 and 3,2 NB-related isomers due to instability of its natural charge-separation of the structures. The latter has the strongest delocalization [118].

To further reliability of the trend, the localized orbital locator integrated π over plane (LOLIPOP) index, is calculated to measure π-stacking ability of aromatic compounds so, this index is related to the optimized geometries. The smaller LOLIPOP the stronger π-stacking (lower π-delocalization). The π-stacking over the ring of second group isostere is stronger due to the presence of three more electronegativity N atoms. From the LOLIPOP results, the NB-pyrrole analogues have smaller values than the parent (pyrrole). This

Table 7
Aromaticity indices for pyrrole and its NB isosteres at B3LYP/6-311 + G (d,p).

Criteria	Magnetic Criteria				Geometry Criteria		Electron delocalization Criteria			
	NICS(0)iso	NICS(0)zz	NICS(1)iso	NICS(1)zz	HOMA	LOLIPOP	FLU	FLU-π	MCI	
									AV1245	NMCBO
Pyrrole	−13.635	−12.384	−10.140	−31.019	0.854	4.562	0.009	0.044	14.481	0.610
First group										
PN2B3	−9.303	−1.290	−7.416	−20.578	0.470	2.430	0.667	0.270	6.042	0.478
PN3B2	−10.512	−2.051	−6.953	−21.904	0.762	3.704	0.015	0.110	7.893	0.545
PN3B4	−11.965	−8.972	−8.509	−27.134	0.782	4.112	1.020	0.026	8.977	0.567
PN2B4	−11.948	−11.031	−9.8253	−28.209	0.639	1.853	1.758	0.292	7.699	0.529
Second group										
PN3,4B2,5	−8.104	6.1307	−5.118	−14.151	0.683	0.201	0.039	0.004	6.378	0.454
PN2,5B3,4	−6.744	3.547	−5.421	−14.695	0.338	0.189	0.083	0.083	0.581	0.397

implies that inorganic system has stronger π-stacking over the ring, lower π-delocalization and lower aromatic character than pyrrole.

3.6.3. Electronic delocalization criteria

The aromatic fluctuation index (FLU) and the FLU-π concerns the number of shared electrons between adjacent atoms and π-atomic valence orbital, respectively. The lower the values of FLU and FLU-π, the stronger the aromaticity. Particularly, the FLU and FLU-π indices give almost the same order of aromaticity for the isosteres analyzed. In the first group, the most stable isosteres **PN3B2 and PN3B4** are more aromatic according to these indices. Furthermore, the most stable isostere in second group (**PN3,4B2,5)** is most aromatic one.

The MCI partition was investigated using normalized multicenter bond order (NMCBO) and AV1245 indices. The larger MCI value the stronger aromaticity within the "atoms-in-molecules" theory [119] and this indicates the electron delocalization capability over a ring is more strong. The greater number of NB unity substituted leads to a decreasing in aromaticity. First group isosteres are more aromatic than second group. In the first group, the **PN3B4** isomer has a slightly higher value and higher electron delocalization 8.977 and 0.567 for AV1245 and NMCBO indices, respectively than the other isosteres. Furthermore, the most stable isostere in the second group (**PN3,4B2,5)** has the most aromatic character.

Thermodynamic stability is often associated with aromaticity of the structures. But, there are many exceptions, the aromaticity is a type of stabilizing factor while energetic stability is affected by others [34,118]. There is a direct relationship between aromaticity and stability.

4. Conclusion

New N–B bond-containing five-membered azaborole analogues were investigated. Two groups make up the isosteric nitrogen boron pyrrole. A NB mono substitution, which only involves the replacement of two carbon atoms (C–C) with N and B atoms, is included in the first group. A total of 12 configurations will result from this substitution. There are only four non-equivalent isosteres left from these twelve variants. There are only two independent isosteres in the second group, which has a total of 6 configurations. The P**N3B2** isostere was more stable than other isosteres in all of the examined azaboroles.

The impacts of mono and double substitution are highlighted by NBO charge and dipole analyses, where the positive charge on carbon and boron atoms attached to nitrogen atom was greater than that on other atoms. The NBO analysis results have been used to provide an explanation for the stabilization interactions that take place inside each replaced ring. Calculations of aromaticity revealed that while all NB isomers have some aromatic properties; they are all less aromatic than pyrrole.

The electrophilic or nucleophilic nature of the structures, the global and local atom-based reactivity characteristics computed using DFT were compatible with the aromatic stabilization. NBO charge and dipole moment analysis effect on typical of mono and double substitution. The NB pyrrole analogues are strong electrophile except **PN3B2** and **PN3B4** isosteres are moderate electrophile. Hence, all NB pyrrole analogues are marginal nucleophile. HOMO and LUMO surfaces and ESP maps are crucial to detect the distribution of the frontier orbitals, and their symmetry.

In summary, we have investigated new five membered azaborole analogues of pyrrole and have studied a lot of their properties. These new structures could be used for material science and pharmaceutical uses.

Author contribution statement

All authors listed have significantly contributed to the development and the writing of this article. Safinaz H. El-Demerdash: Conceived and designed the experiments; Analyzed and interpreted the data; Wrote the Paper. Shaimaa F. Gad: Performed the experiments; Wrote the Paper. Ibrahim M. El-Mehasseb: Contributed reagents, materials, analysis tools or data. Khaled E. El-Kelany: Analyzed and interpreted the data; Wrote the Paper.

Data availability statement

Data included in article/supp. Material/referenced in article.

Additional information

No additional information is available for this paper.

Funding

This research has no funding.

Ethics approval

Authors certify that they follow the journal ethics to the best of their knowledge.

Consent to participate

Authors certify the Consent.

Consent for publication

Authors certify the Consent.

Declaration of competing interest

The authors declare that they have no known competing financial interests or personal relationships that could have appeared to influence the work reported in this paper.

References

[1] C.W. Thornber, Isosterism and molecular modification in drug design, Chem. Soc. Rev. 8 (1979) 563–580, https://doi.org/10.1039/CS9790800563.
[2] A.J.L. Catão, A. López-Castillo, Stability and molecular properties of the boron-nitrogen alternating analogs of azulene and naphthalene: a computational study, J. Mol. Model. 23 (2017), https://doi.org/10.1007/s00894-017-3279-y.
[3] W.H. Moon, M.S. Son, H.J. Hwang, Theoretical study on structure of boron nitride fullerenes, Appl. Surf. Sci. 253 (2007) 7078–7081, https://doi.org/10.1016/j.apsusc.2007.02.047.
[4] F. Li, J. Lu, G. Tan, M. Ma, X. Wang, H. Zhu, Boron nitride nanotubes composed of four- and eight-membered rings, Phys. Lett. Sect. A Gen. At. Solid State Phys. 383 (2019) 76–82, https://doi.org/10.1016/j.physleta.2018.09.012.
[5] E. Vessally, P. Farajzadeh, E. Najafi, Possible sensing ability of boron nitride nanosheet and its al– and si–doped derivatives for methimazole drug by computational study, Iran, J. Chem. Chem. Eng. 40 (2021) 1001–1011, https://doi.org/10.30492/ijcce.2021.141635.4498.
[6] M.J.D. Bosdet, W.E. Piers, B-N as a C-C substitute in aromatic systems, Can, J. Chem. 87 (2009) 8–29, https://doi.org/10.1139/V08-110.
[7] P.G. Campbell, A.J.V. Marwitz, S.Y. Liu, Recent advances in azaborine chemistry, Angew. Chem., Int. Ed. 51 (2012) 6074–6092, https://doi.org/10.1002/anie.201200063.
[8] X.Y. Wang, J.Y. Wang, J. Pei, BN heterosuperbenzenes: synthesis and properties, Chem. Eur J. 21 (2015) 3528–3539, https://doi.org/10.1002/chem.201405627.
[9] H. Helten, B=N units as part of extended π-conjugated oligomers and polymers, Chem. Eur J. 22 (2016) 12972–12982, https://doi.org/10.1002/chem.201602665.
[10] Z.X. Giustra, S.Y. Liu, The state of the art in azaborine chemistry: new synthetic methods and applications, J. Am. Chem. Soc. 140 (2018) 1184–1194, https://doi.org/10.1021/jacs.7b09446.
[11] M.K. Kesharwani, M. Suresh, A. Das, B. Ganguly, Borazine as a sensor for fluoride ion: a computational and experimental study, Tetrahedron Lett. 52 (2011) 3636–3639, https://doi.org/10.1016/j.tetlet.2011.05.018.
[12] Y. Song, C. Zhang, B. Li, G. Ding, D. Jiang, H. Wang, X. Xie, Van der Waals epitaxy and characterization of hexagonal boron nitride nanosheets on graphene, Nanoscale Res. Lett. 9 (2014) 1–7, https://doi.org/10.1186/1556-276X-9-367.
[13] L. de Abreu, A. López-Castillo, Theoretical characterization of the BN and BP coronenes by IR, Raman, and UV-VIS spectra, J. Chem. Phys. 137 (2012), 13207, https://doi.org/10.1063/1.4737519.
[14] D. Golberg, Y. Bando, K. Kurashima, T. Sato, Synthesis and characterization of ropes made of BN multiwalled nanotubes, Scripta Mater. 44 (2001) 1561–1565, https://doi.org/10.1016/S1359-6462(01)00724-2.
[15] T. Ishii, T. Sato, Y. Sekikawa, M. Iwata, Growth of whiskers of hexagonal boron nitride, J. Cryst. Growth 52 (1981) 285–289, https://doi.org/10.1016/0022-0248(81)90206-2.
[16] A.H. Tavakoli, J.A. Golczewski, J. Bill, A. Navrotsky, Effect of boron on the thermodynamic stability of amorphous polymer-derived Si-(B-)-CN ceramics, Acta Mater. 60 (2012) 4514–4522, https://doi.org/10.1016/j.actamat.2012.05.010.
[17] A. Lõpez-Castillo, Prediction of boron-phosphorous nanographene-like material, Int. J. Quant. Chem. 112 (2012) 3152–3157, https://doi.org/10.1002/qua.24096.
[18] Q.L. Almas, J.K. Pearson, Novel bonding mode in phosphine haloboranes, ACS Omega 3 (2018) 608–614, https://doi.org/10.1021/acsomega.7b01529.
[19] D.H. Knack, J.L. Marshall, G.P. Harlow, A. Dudzik, M. Szaleniec, S.Y. Liu, J. Heider, BN/CC isosteric compounds as enzyme inhibitors: N- and B-ethyl-1,2-azaborine inhibit ethylbenzene hydroxylation as nonconvertible substrate analogues, Angew. Chem., Int. Ed. 52 (2013) 2599–2601, https://doi.org/10.1002/anie.201208351.
[20] M.E. Bluhm, M.G. Bradley, R. Butterick, U. Kusari, L.G. Sneddon, Enhanced ammonia borane dehydrogenation in ionic liquids, ACS Natl. Meet. B. Abstr. 232 (2006) 7748–7749.
[21] Q. Weng, X. Wang, C. Zhi, Y. Bando, D. Golberg, Boron nitride porous microbelts for hydrogen storage, ACS Nano 7 (2013) 1558–1565, https://doi.org/10.1021/nn305320v.
[22] X. Chen, X.P. Gao, H. Zhang, Z. Zhou, W.K. Hu, G.L. Pan, H.Y. Zhu, T.Y. Yan, D.Y. Song, Preparation and electrochemical hydrogen storage of boron nitride nanotubes, J. Phys. Chem. B 109 (2005) 11525–11529, https://doi.org/10.1021/jp050105u.
[23] P.G. Campbell, L.N. Zakharov, D.J. Grant, D.A. Dixon, S.Y. Liu, Hydrogen storage by boron-nitrogen heterocycles: a simple route for spent fuel regeneration, J. Am. Chem. Soc. 132 (2010) 3289–3291, https://doi.org/10.1021/ja9106622.
[24] G. Chen, L.N. Zakharov, M.E. Bowden, A.J. Karkamkar, S.M. Whittemore, E.B. Garner, T.C. Mikulas, D.A. Dixon, T. Autrey, S.Y. Liu, Bis-BN cyclohexane: a remarkably kinetically stable chemical hydrogen storage material, J. Am. Chem. Soc. 137 (2015) 134–137, https://doi.org/10.1021/ja511766p.
[25] X. Wang, F. Zhang, J. Liu, R. Tang, Y. Fu, D. Wu, Q. Xu, X. Zhuang, G. He, X. Feng, Ladder-type BN-embedded heteroacenes with blue emission, Org. Lett. 15 (2013) 5714–5717, https://doi.org/10.1021/ol402745r.
[26] X.Y. Wang, F.D. Zhuang, R.B. Wang, X.C. Wang, X.Y. Cao, J.Y. Wang, J. Pei, A straightforward strategy toward large BN-embedded π-systems: synthesis, structure, and optoelectronic properties of extended BN heterosuperbenzenes, J. Am. Chem. Soc. 136 (2014) 3764–3767, https://doi.org/10.1021/ja500117z.
[27] G. Li, Y. Zhao, J. Li, J. Cao, J. Zhu, X.W. Sun, Q. Zhang, Synthesis, characterization, physical properties, and OLED application of single BN-fused perylene diimide, J. Org. Chem. 80 (2015) 196–203, https://doi.org/10.1021/jo502296z.
[28] S. Xu, Y. Zhang, B. Li, S.Y. Liu, Site-selective and stereoselective trans-hydroboration of 1,3-enynes catalyzed by 1,4-azaborine-based phosphine-Pd complex, J. Am. Chem. Soc. 138 (2016) 14566–14569, https://doi.org/10.1021/jacs.6b09759.
[29] S. Tsuchiya, H. Saito, K. Nogi, H. Yorimitsu, Aromatic metamorphosis of indoles into 1,2-benzazaborins, Org. Lett. 21 (2019) 3855–3860, https://doi.org/10.1021/acs.orglett.9b01353.
[30] E.R. Abbey, L.N. Zakharov, S.Y. Liu, Electrophilic aromatic substitution of a BN indole, J. Am. Chem. Soc. 132 (2010) 16340–16342, https://doi.org/10.1021/ja107312u.
[31] E.R. Abbey, L.N. Zakharov, S.Y. Liu, Boron in disguise: the parent fused BN indole, J. Am. Chem. Soc. 133 (2011) 11508–11511, https://doi.org/10.1021/ja205779b.

[32] C.J. Johnson, R.W. Zoellner, The smallest borazine-fused cyclacenes: novel N-H conformations in cyclo-BN-anthracene and cyclo-BN-tetracene from Hartree-Fock and density functional calculations, J. Mol. Struct. THEOCHEM. 893 (2009) 9–16, https://doi.org/10.1016/j.theochem.2008.09.012.

[33] I. Rozas, I. Alkorta, J. Elguero, Behavior of ylides containing N, O, and C atoms as hydrogen bond acceptors, J. Am. Chem. Soc. 122 (2000) 11154–11161, https://doi.org/10.1021/ja0017864.

[34] D. Ghosh, G. Periyasamy, S.K. Pati, Density functional theoretical investigation of the aromatic nature of BN substituted benzene and four ring polyaromatic hydrocarbons, Phys. Chem. Chem. Phys. 13 (2011) 20627–20636, https://doi.org/10.1039/c1cp22104c.

[35] F. Sagan, R. Filas, M.P. Mitoraj, Non-covalent interactions in hydrogen storage materials LiN(CH3)2BH3 and KN(CH3)2BH3, Crystals 6 (2016) 11–23, https://doi.org/10.3390/cryst6030028.

[36] C. Ma, J. Zhang, J. Li, C. Cui, Multiple C-H borylation of phenylhydrazones to boron-nitrogen analogues of benzopentalene, Chem. Commun. 51 (2015) 5732–5734, https://doi.org/10.1039/c5cc00471c.

[37] R.C. Bakus, D.A. Atwood, Boron-nitrogen CompoundsBased in Part on the Article Boron-Nitrogen Compounds by Robert T. Paine Which Appeared in the Encyclopedia of Inorganic Chemistry, Encycl. Inorg. Bioinorg. Chem., 2011, https://doi.org/10.1002/9781119951438.eibc0026.

[38] X.Y. Wang, A. Narita, X. Feng, K. Müllen, B2N2-Dibenzo[a,e]pentalenes: effect of the BN Orientation Pattern on Antiaromaticity and Optoelectronic Properties, J. Am. Chem. Soc. 137 (2015) 7668–7671, https://doi.org/10.1021/jacs.5b05056.

[39] A.M. Rouf, J. Wu, J. Zhu, Probing a general rule towards thermodynamic stabilities of mono BN-doped lower polyenes, Chem. Asian J. 12 (2017) 605–614, https://doi.org/10.1002/asia.201601753.

[40] J.S.A. Ishibashi, A. Dargelos, C. Darrigan, A. Chrostowska, S.Y. Liu, BN tetracene: extending the reach of BN/CC isosterism in acenes, Organometallics 36 (2017) 2494–2497, https://doi.org/10.1021/acs.organomet.7b00296.

[41] R.C. Fortenberry, Methylidyne-replaced boron nitride fullerenes and nanotubes: a wave function study, New J. Chem. 40 (2016) 8149–8157, https://doi.org/10.1039/c6nj01821a.

[42] A.F. Sattarova, Y.N. Biglova, A.G. Mustafin, Quantum-chemical approaches in the study of fullerene and its derivatives by the example of the most typical cycloaddition reactions: a review, Int. J. Quant. Chem. 122 (2022) 1–30, https://doi.org/10.1002/qua.26863.

[43] L.S. Panchakarla, A. Govindaraj, C.N.R. Rao, Nitrogen- and boron-doped double- Walled carbon nanotubes, ACS Nano 1 (2007) 494–500, https://doi.org/10.1021/nn700230n.

[44] A. Abengózar, P. García-García, M.A. Fernández-Rodríguez, D. Sucunza, J.J. Vaquero, Recent Developments in the Chemistry of BN-Aromatic Hydrocarbons, Elsevier Inc., 2021, https://doi.org/10.1016/bs.aihch.2021.01.001.

[45] V.A. Dixit, W.R.F. Goundry, S. Tomasi, CC/B-N substitution in five membered heterocycles. A computational analysis, New J. Chem. 41 (2017) 3619–3633, https://doi.org/10.1039/c7nj00950j.

[46] S.C. Philkhana, F.O. Badmus, I.C. Dos Reis, R. Kartika, Recent advancements in pyrrole synthesis, Synth. Met. 53 (2021) 1531–1555, https://doi.org/10.1055/s-0040-1706713.

[47] A.B. Trofimov, I.L. Zaitseva, T.E. Moskovskaya, N.M. Vitkovskaya, Theoretical investigation of photoelectron spectra of furan, pyrrole, thiophene, and selenole, Chem. Heterocycl. Compd. 44 (2008) 1101–1112, https://doi.org/10.1007/s10593-008-0159-5.

[48] V. Bhardwaj, D. Gumber, V. Abbot, S. Dhiman, P. Sharma, Pyrrole: a resourceful small molecule in key medicinal hetero-aromatics, RSC Adv. 5 (2015) 15233–15266, https://doi.org/10.1039/c4ra15710a.

[49] M.J. Frisch, G.W. Trucks, H.B. Schlegel, G.E. Scuseria, M.A. Robb, J.R. Cheeseman, G. Scalmani, V. Barone, B. Mennucci, G.A. Petersson, H. Nakatsuji, M. Caricato, X. Li, H.P. Hratchian, A.F. Izmaylov, J. Bloino, G. Zheng, J.L. Sonnenberg, M. Hada, M. Ehara, K. Toyota, R. Fukuda, J. Hasegawa, M. Ishida, T. Nakajima, Y. Honda, O. Kitao, H. Nakai, T. Vreven, J.A. Montgomery, J.E. Peralta, F. Ogliaro, M. Bearpark, J.J. Heyd, E. Brothers, K.N. Kudin, V. N. Staroverov, R. Kobayashi, J. Normand, K. Raghavachari, A. Rendell, J.C. Burant, S.S. Iyengar, J. Tomasi, M. Cossi, N. Rega, J.M. Millam, M. Klene, J. E. Knox, J.B. Cross, V. Bakken, C. Adamo, J. Jaramillo, R. Gomperts, R.E. Stratmann, O. Yazyev, A.J. Austin, R. Cammi, C. Pomelli, J.W. Ochterski, R.L. Martin, K. Morokuma, V.G. Zakrzewski, G.A. Voth, P. Salvador, J.J. Dannenberg, S. Dapprich, A.D. Daniels, Farkas, J.B. Foresman, J. V Ortiz, J. Cioslowski, D.J. Fox, Gaussian 09, Revision B.01, Gaussian 09, Revis. B.01, Gaussian, Inc., Wallingford CT, 2009, pp. 1–20, citeulike-article-id:9096580.

[50] Version 5 GaussView, R. Dennington, T. Keith, J. Millam, Semichem Inc, Shawnee Mission KS, 2009.

[51] http://www.chemcraftprog.com.

[52] A.D. Becke, Density-functional thermochemistry. III. The role of exact exchange, J. Chem. Phys. 98 (1993) 5648–5652, https://doi.org/10.1063/1.464913.

[53] C. Lee, W. Yang, R.G. Parr, Development of the Colle-Salvetti correlation-energy formula into a functional of the electron density, Phys. Rev. B 37 (1988) 785–789, https://doi.org/10.1103/PhysRevB.37.785.

[54] N. Farrell, Common ground, clever girls autoethnographies class, Gend. Ethn 115–123 (2019), https://doi.org/10.1007/978-3-030-29658-2_6.

[55] J.A. Montgomery, M.J. Frisch, J.W. Ochterski, G.A. Petersson, A complete basis set model chemistry. VI. Use of density functional geometries and frequencies, J. Chem. Phys. 110 (1999) 2822–2827, https://doi.org/10.1063/1.477924.

[56] M.C. Flores, E.A. Márquez, J.R. Mora, Molecular modeling studies of bromopyrrole alkaloids as potential antimalarial compounds: a DFT approach, Med. Chem. Res. 27 (2018) 844–856, https://doi.org/10.1007/s00044-017-2107-3.

[57] V.R. Mishra, N. Sekar, Photostability of coumarin laser dyes - a mechanistic study using global and local reactivity descriptors, J. Fluoresc. 27 (2017) 1101–1108, https://doi.org/10.1007/s10895-017-2045-y.

[58] S. Das, S.V. Shedge, S. Pal, Critical study of the charge transfer parameter for the calculation of interaction energy using the local hard-soft acid-base principle, J. Phys. Chem. A 117 (2013) 10933–10943, https://doi.org/10.1021/jp407070h.

[59] T. Koopmans, Über die Zuordnung von Wellenfunktionen und Eigenwerten zu den Einzelnen Elektronen Eines Atoms, Physica 1 (1934) 104–113.

[60] T. Lu, F. Chen, Multiwfn: a multifunctional wavefunction analyzer, J. Comput. Chem. 33 (2012) 580–592, https://doi.org/10.1002/jcc.22885.

[61] F.E.D. Glendening, A.E. Reed, J.E. Carpenter, Weinhold, NBO Version 3.1, Gaussian Inc., Pittsburgh., 2003.

[62] M. Randic, Aromaticity of polycyclic conjugated hydrocarbons, ChemInform 34 (2003), https://doi.org/10.1002/chin.200348275.

[63] V.D. Khavryuchenko, O.V. Khavryuchenko, Y.A. Tarasenko, V.V. Lisnyak, Computer simulation of N-doped polyaromatic hydrocarbons clusters, Chem. Phys. 352 (2008) 231–234, https://doi.org/10.1016/j.chemphys.2008.06.019.

[64] J.E. Del Bene, M. Yáez, I. Alkorta, J. Elguero, An ab initio study of the structures and selected properties of 1,2-dihydro-1,2-azaborine and related molecules, J. Chem. Theor. Comput. 5 (2009) 2239–2247, https://doi.org/10.1021/ct900128v.

[65] J. Poater, X. Fradera, M. Duran, M. Solà, The delocalization index as an electronic aromaticity criterion: application to a series of planar polycyclic aromatic hydrocarbons, Chem. Eur J. 9 (2003) 400–406, https://doi.org/10.1002/chem.200390041.

[66] J.A.N.F. Gomes, R.B. Mallion, ChemInform abstract: aromaticity and ring currents, ChemInform 32 (2010), https://doi.org/10.1002/chin.200131294.

[67] R.W.A. Havenith, F. Lugli, P.W. Fowler, E. Steiner, Ring current patterns in annelated bicyclic polyenes, J. Phys. Chem. A 106 (2002) 5703–5708, https://doi.org/10.1021/jp0204962.

[68] P.V.R. Schleyer, C. Maerker, A. Dransfeld, H. Jiao, N.J.R. Van Eikema Hommes, Nucleus-independent chemical shifts: a simple and efficient aromaticity probe, J. Am. Chem. Soc. 118 (1996) 6317–6318, https://doi.org/10.1021/ja960582d.

[69] Z. Chen, C.S. Wannere, C. Corminboeuf, R. Puchta, P. von Ragué Schleyer, Nucleus-independent chemical shifts (NICS) as an aromaticity criterion, Chem. Rev. 105 (2005) 3842–3888, https://doi.org/10.1021/cr030088+.

[70] I. Pérez-Juste, M. Mandado, L. Carballeira, Contributions from orbital-orbital interactions to nucleus-independent chemical shifts and their relation with aromaticity or antiaromaticity of conjugated molecules, Chem. Phys. Lett. 491 (2010) 224–229, https://doi.org/10.1016/j.cplett.2010.03.077.

[71] T.M. Krygowski, M. Cyrański, Separation of the energetic and geometric contributions to the aromaticity. Part IV. A general model for the π-electron systems, Tetrahedron 52 (1996) 10255–10264, https://doi.org/10.1016/0040-4020(96)00560-1.

[72] T.M. Krygowski, M.K. Cyrański, Structural aspects of aromaticity, Chem. Rev. 101 (2001) 1385–1419, https://doi.org/10.1021/cr990326u.

[73] J.F. Gonthier, S.N. Steinmann, L. Roch, A. Ruggi, N. Luisier, K. Severin, C. Corminboeuf, π-Depletion as a criterion to predict π-stacking ability, Chem. Commun. 48 (2012) 9239–9241, https://doi.org/10.1039/c2cc33886f.

[74] J. Poater, M. Duran, M. Solà, B. Silvi, Theoretical evaluation of electron delocalization in aromatic molecules by means of atoms in molecules (AIM) and electron localization function (ELF) topological approaches, Chem. Rev. 105 (2005) 3911–3947, https://doi.org/10.1021/cr030085x.
[75] E. Matito, M. Duran, M. Solà, The aromatic fluctuation index (FLU): a new aromaticity index based on electron delocalization, J. Chem. Phys. 122 (2005), https://doi.org/10.1063/1.1824895.
[76] M. Giambiagi, M.S. De Giambiagi, C.D. Dos Santos Silva, A.P. De Figueiredo, Multicenter bond indices as a measure of aromaticity, Phys. Chem. Chem. Phys. 2 (2000) 3381–3392, https://doi.org/10.1039/b002009p.
[77] P. Bultinck, R. Ponec, S. Van Damme, Multicenter bond indices as a new measure of aromaticity in polycyclic aromatic hydrocarbons, J. Phys. Org. Chem. 18 (2005) 706–718, https://doi.org/10.1002/poc.922.
[78] R. Bochicchio, R. Ponec, A. Torre, L. Lain, Multicenter bonding within the AIM theory, Theor. Chem. Acc. 105 (2001) 292–298, https://doi.org/10.1007/s002140000236.
[79] M. Serhan, M. Sprowls, D. Jackemeyer, M. Long, I.D. Perez, W. Maret, N. Tao, E. Forzani, Total iron measurement in human serum with a smartphone, AIChE Annu. Meet. Conf. Proc. 2019-Novem (2019), https://doi.org/10.1039/x0xx00000x.
[80] P. Bultinck, M. Rafat, R. Ponec, B. Van Gheluwe, R. Carbó-Dorca, P. Popelier, Electron delocalization and aromaticity in linear polyacenes: atoms in molecules multicenter delocalization index, J. Phys. Chem. A 110 (2006) 7642–7648, https://doi.org/10.1021/jp0609176.
[81] F. Weinhold, C.R. Landis, A.E. Reed, F. Weinhold, Intermolecular interactions from a natural bond orbital , donor-acceptor viewpoint intermolecular interactions from a natural bond orbital , donor-acceptor viewpoint, Chem. Educ. Res. Pract. 2 (2001) 91–104.
[82] A.E. Reed, R.B. Weinstock, F. Weinhold, Natural population analysis, J. Chem. Phys. 83 (1985) 735–746, https://doi.org/10.1063/1.449486.
[83] E. Matito, An electronic aromaticity index for large rings, Phys. Chem. Chem. Phys. 18 (2016) 11839–11846, https://doi.org/10.1039/c6cp00636a.
[84] B.I. Łydzba-Kopczyńska, K.B. Beć, J. Tomczak, J.P. Hawranek, Optical constants of liquid pyrrole in the infrared, J. Mol. Liq. 172 (2012) 34–40, https://doi.org/10.1016/j.molliq.2012.05.009.
[85] W. Kasten, H. Dreizler, R.L. Kuczkowski, Boron and nitrogen hyperfine structure in the microwave spectrum of trimethylamine-borane, Zeitschrift Fur Naturforsch. - Sect. A J. Phys. Sci. 40 (1985) 1262–1264, https://doi.org/10.1515/zna-1985-1212.
[86] R. Dinda, O. Ciobanu, H. Wadepohl, O. Hübner, R. Acharyya, H.J. Himmel, Synthesis and structural characterization of a stable dimeric boron(II) dication, Angew. Chem., Int. Ed. 46 (2007) 9110–9113, https://doi.org/10.1002/anie.200703616.
[87] A. Haaland, Covalent versus dative bonds to main group metals, a useful distinction, Angew Chem. Int. Ed. Engl. 28 (1989) 992–1007, https://doi.org/10.1002/anie.198909921.
[88] D.K. Straub, Lewis structures of boron compounds involving multiple bonding, J. Chem. Educ. 73 (1995) 494–497, https://doi.org/10.1021/ed072p494.
[89] J.J. Engelberts, R.W.A. Havenith, J.H. Van Lenthe, L.W. Jenneskens, P.W. Fowler, The electronic structure of inorganic benzenes: valence bond and ring-current descriptions, Inorg. Chem. 44 (2005) 5266–5272, https://doi.org/10.1021/ic050017o.
[90] N. Matsunaga, S.G. Mark, Stabilities and energetics of inorganic benzene isomers: prismanes, J. Am. Chem. Soc. 116 (1994) 11407–11419, https://doi.org/10.1021/ja00104a021.
[91] S. Dheivamalar, K. Bansura Banu, The adsorption mechanism, structural and electronic properties of pyrrole adsorbed ZnO nano clusters in the field photovoltaic cells by density functional theory, Indian J. Pure Appl. Phys. 57 (2019) 713–724.
[92] L. Ahmed, R. Omer, 1H-Pyrrole-Furan-Thiophene molecule corrosion inhibitor behaviors, Mater. Phys. Chem. & Funct 4 (2021) 1–4, https://doi.org/10.54565/jphcfum.989851.
[93] H.F. Hizaddin, R. Anantharaj, M.A. Hashim, A quantum chemical study on the molecular interaction between pyrrole and ionic liquids, J. Mol. Liq. 194 (2014) 20–29, https://doi.org/10.1016/j.molliq.2013.12.041.
[94] G. Gece, The use of quantum chemical methods in corrosion inhibitor studies, Corrosion Sci. 50 (2008) 2981–2992, https://doi.org/10.1016/j.corsci.2008.08.043.
[95] R.A. Costa, E.S.A. Junior, J.D.A. Bezerra, J.M. Mar, E.S. Lima, M.L.B. Pinheiro, D.V.C. Mendonça, G.B.P. Lopes, A.D.S. Branches, K.M.T. Oliveira, Theoretical investigation of the structural, spectroscopic, electronic, and pharmacological properties of 4-nerolidylcathecol, an important bioactive molecule, J. Chem. 2019 (2019) 18–22, https://doi.org/10.1155/2019/9627404.
[96] R. Vijayaraj, V. Subramanian, P.K. Chattaraj, Comparison of global reactivity descriptors calculated using various density functionals: a QSAR perspective, J. Chem. Theor. Comput. 5 (2009) 2744–2753, https://doi.org/10.1021/ct900347f.
[97] L. Sinha, O. Prasad, V. Narayan, S.R. Shukla, Raman, FT-IR spectroscopic analysis and first-order hyperpolarisability of 3-benzoyl-5-chlorouracil by first principles, Mol. Simulat. 37 (2011) 153–163, https://doi.org/10.1080/08927022.2010.533273.
[98] S.J. Grabowski, J. Leszczynski, Unrevealing the Nature of Hydrogen Bonds: π-electron Delocalization Shapes H-Bond Features: Intramolecular and Intermolecular Resonance-Assisted Hydrogen Bonds, Hydrog. Bond. - New Insights, 2006, pp. 487–512, https://doi.org/10.1007/978-1-4020-4853-1_14.
[99] R.G. Pearson, Hard and soft acids and bases, J. Am. Chem. Soc. 85 (1963) 3533–3539, https://doi.org/10.1021/ja00905a001.
[100] G. Shanmugam, Identification of Potential Nematicidal Compounds against the Pine Wood Nematode, Bursaphelenchus, 2018, https://doi.org/10.3390/molecules23071828.
[101] L.R. Domingo, R. Mar, A Molecular Electron Density Theory Study of the, 4, 2017, https://doi.org/10.3390/molecules22050750.
[102] A. Madanagopal, S. Periandy, P. Gayathri, S. Ramalingam, S. Xavier, V.K. Ivanov, Spectroscopic and computational investigation of the structure and pharmacological activity of 1-benzylimidazole, J. Taibah Univ. Sci. 11 (2017) 975–996, https://doi.org/10.1016/j.jtusci.2017.02.006.
[103] C. Pigot, F. Dumur, Molecular engineering in 2D surface covalent organic frameworks: towards next generation of molecular tectons - a mini review, Synth. Met. 260 (2020), 116265, https://doi.org/10.1016/j.synthmet.2019.116265.
[104] R. Perez, Discriminating chemical bonds, Science 337 (80) (2012) 1305–1306, https://doi.org/10.1126/science.1227726.
[105] D.G. De Oteyza, P. Gorman, Y.C. Chen, S. Wickenburg, A. Riss, D.J. Mowbray, G. Etkin, Z. Pedramrazi, H.Z. Tsai, A. Rubio, M.F. Crommie, F.R. Fischer, Direct imaging of covalent bond structure in single-molecule chemical reactions, Science 340 (80) (2013) 1434–1437, https://doi.org/10.1126/science.1238187.
[106] L.R. Domingo, Molecular electron density theory: a modern view of reactivity in organic chemistry, Molecules 21 (2016) 1–15, https://doi.org/10.3390/molecules21101319.
[107] P. Lazzeretti, Assessment of aromaticity via molecular response properties, Phys. Chem. Chem. Phys. 6 (2004) 217–223, https://doi.org/10.1039/b311178d.
[108] T.M. Krygowski, K. Ejsmont, B.T. Stepień, M.K. Cyrański, J. Poater, M. Solà, Relation between the substituent effect and aromaticity, J. Org. Chem. 69 (2004) 6634–6640, https://doi.org/10.1021/jo0492113.
[109] T.M. Krygowski, B.T. Stępień, M.K. Cyrański, K. Ejsmont, Relation between resonance energy and substituent resonance effect in P-phenols, J. Phys. Org. Chem. 18 (2005) 886–891, https://doi.org/10.1002/poc.960.
[110] D. Inostroza, V. García, O. Yañez, J.J. Torres-Vega, A. Vásquez-Espinal, R. Pino-Rios, R. Báez-Grez, W. Tiznado, On the NICS limitations to predict local and global current pathways in polycyclic systems, New J. Chem. 45 (2021) 8345–8351, https://doi.org/10.1039/d1nj01510a.
[111] R. Báez-Grez, W.A. Rabanal-León, L. Alvarez-Thon, L. Ruiz, W. Tiznado, R. Pino-Rios, Aromaticity in heterocyclic analogues of benzene: dissected NICS and current density analysis, J. Phys. Org. Chem. 32 (2019) 1–7, https://doi.org/10.1002/poc.3823.
[112] K.E. Horner, P.B. Karadakov, Chemical bonding and aromaticity in furan, pyrrole, and thiophene: a magnetic shielding study, J. Org. Chem. 78 (2013) 8037–8043, https://doi.org/10.1021/jo401319k.
[113] K. Najmidin, A. Kerim, P. Abdirishit, H. Kalam, T. Tawar, A comparative study of the aromaticity of pyrrole, furan, thiophene, and their aza-derivatives, J. Mol. Model. 19 (2013) 3529–3535, https://doi.org/10.1007/s00894-013-1877-x.
[114] K.K. Zborowski, J. Poater, Pyrrole and pyridine in the water environment—effect of discrete and continuum solvation models, ACS Omega 6 (2021) 24693–24699, https://doi.org/10.1021/acsomega.1c03437.
[115] M.M. Meshhal, M.F. Shibl, S.H. El-Demerdash, A.M. El-Nahas, A computational study on molecular structure and stability of tautomers of dipyrrole-based phenanthroline analogue, Comput. Theor. Chem. 1145 (2018) 6–14, https://doi.org/10.1016/j.comptc.2018.10.003.

[116] A.B. El-Meligy, S.H. El-Demerdash, M.A. Abdel-Rahman, M.A.M. Mahmoud, T. Taketsugu, A.M. El-Nahas, Structures, energetics, and spectra of (NH) and (OH) tautomers of 2-(2-Hydroxyphenyl)-1-azaazulene: a density functional theory/time-dependent density functional theory study, ACS Omega 7 (2022) 14222–14238, https://doi.org/10.1021/acsomega.2c00866.
[117] C.P. Frizzo, M.A.P. Martins, Aromaticity in heterocycles: new HOMA index parametrization, Struct. Chem. 23 (2012) 375–380, https://doi.org/10.1007/s11224-011-9883-z.
[118] M. Baranac-Stojanović, Aromaticity and stability of azaborines, Chem. Eur J. 20 (2014) 16558–16565, https://doi.org/10.1002/chem.201402851.
[119] M. Giambiagi, M.S. de Giambiagi, K.C. Mundim, Definition of a multicenter bond index, Struct. Chem. 1 (1990) 423–427, https://doi.org/10.1007/BF00671228.